J. Electrochem. Sci. Eng. **00(0)** (2024) 000-000; http://dx.doi.org/10.5599/jese.2257

Open Access : : ISSN 1847-9286
www.jESE-online.org

Original scientific paper

Characteristics of graphite obtained by recycling lithium - iron phosphate batteries

Ivan Shcherbatiuk[1], Hanna Potapenko[1,2], Danylo Panchenko[1], Volodymyr Khomenko[3,4], Dmytro Patlun[4], Borys Haliuk[3], Roman Derkach[2], Oleksandr Potapenko[1,3] and Viacheslav Barsukov[3,✉]

[1]*Joint Department of Electrochemical Energy Systems of National Academy of Science of Ukraine, Vernadsky ave., 38-A, Kyiv, 03142, Ukraine*

[2]*Faculty of Materials Metallurgy and Chemistry, Jiangxi University of Science and Technology, Ganzhou, 341000, China*

[3]*Institute for Sorption and Problems of Endoecology of National Academy of Science of Ukraine, 13, Generala Naumova str., Kyiv 03164 Ukraine*

[4]*Kyiv National University of Technologies and Design, Mala Shyianovska (Nemyrovycha-Danchenka) Street, 2, Kyiv 01011, Ukraine*

Corresponding authors: ✉ *v-barsukov@i.ua Tel.: +380 67 504 4565; Fax: +380 44 594 0139*

Received: January 27, 2024; Accepted: March 27, 2024; Published: April 27, 2024

Abstract

Based on both the economic and environmental points of view, processing used lithium-ion batteries (LIBs) is of great importance. The valuable components contained in LIB (cathode, anode and current collectors) generate high interest in solving the problem of resource deficiency and reducing environmental destruction due to overexploitation. The starting anode material extracted from a used lithium iron phosphate battery is a mixture of graphite, acetylene carbon black, and polymer binder. Reusing this material in lithium batteries without additional cleaning is impractical owing to poor electrochemical characteristics and the presence of impurities. To achieve effective regeneration, the recycled anode material is first treated in a nitric acid solution to remove copper foil and lithium ions with electrolyte interaction products formed during battery operation. The next step is heat treatment of the material, which allows the removal of acetylene soot and polymer glue binder. The tests showed sufficiently high values of the specific capacity of recycled graphite (~330 mA h g^{-1} at 0.1 C), which are comparable to commercial materials and meet the requirements of reuse.

Keywords

Lithium-ion batteries; recycling; graphite anode; electrochemical parameters; impedance

Introduction

In the context of global population growth to seven billion people, it is projected that electricity production will need to be doubled by the middle of the 21st century to ensure a stable standard of living [1-3]. The problem of increasing the volume of electricity is complex, given that most of the energy is currently generated from non-renewable sources. This causes significant carbon dioxide emissions. Therefore, it is important to focus on the development of renewable energy sources such as wind, solar, tidal and geothermal energy. This involves innovation in the areas of electricity generation and storage, where batteries are becoming a key element in an alternative energy strategy.

Since Sony's first commercial introduction of lithium-ion batteries (LIBs) in 1990, they have been widely adopted. LIBs have a successful combination of energy density, durability, and convenience, making them a popular choice for a wide range of devices and applications.

The global demand for LIB is predicted to approach 3600 GWh by 2030 (Figure 1) [4]. The global production capacity market shares of <1 % today for Europe and USA could increase greatly in the future. By 2030, both regions could reach 5-6 % global shares. In total, the forecasts for the development of production capacities for graphite as an anode material amount to about 4 million tons by 2027/2028. However, the most startling feature in global battery cell manufacturing is the dominance of Asian companies and the localization of production in China because more than half of the declared production capacities are located in Asia. However, by 2030, around one-quarter of cell production could be sited in Europe and around one-fifth in the USA. In a similar manner, half of the production capacities are made by Chinese companies. Moreover, the announcements of Korean companies are the same as the sum of all potential European battery cell fabricators [5-7].

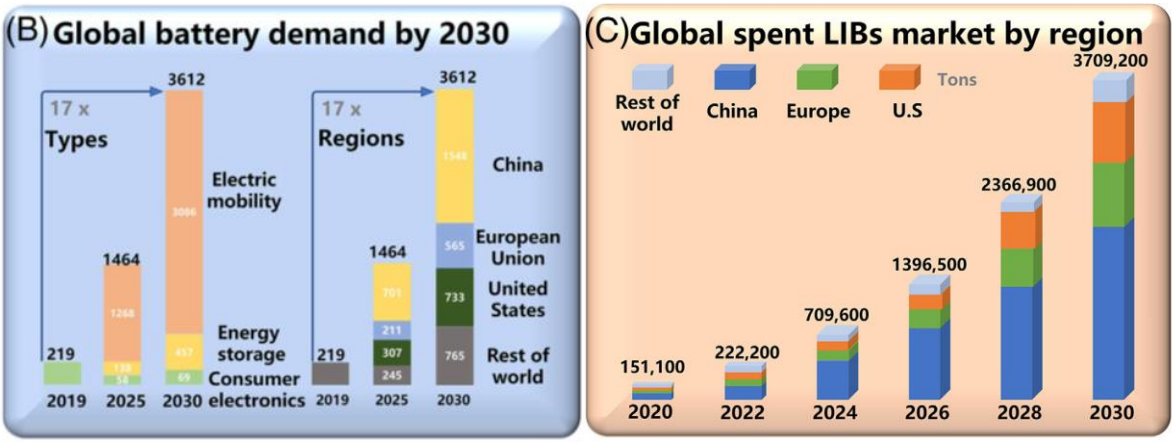

Figure 1. *Projected global demand for batteries until 2030 (B) and the global market for spent lithium-ion batteries (C). (Reprint from [4] The Creative Commons Attribution License from Wiley)*

From both economic and environmental points of view, the processing of used LIBs is of great importance. The valuable components contained in LIB (cathode, anode and current collectors) can make a significant contribution to solving the problem of resource scarcity [8,9] and reducing environmental destruction due to overexploitation.

Graphite is used as the primary anode material in most commercial LIBs. Other anode materials, such as silicon, tin, amorphous carbon, and lithium titanite-based anode, account for only about 9 % [10]. The advantages of a graphite anode include high cycling stability, capacity, and low price [11].

Due to the increase in the production of electric vehicles, there may be a shortage of materials for making batteries over the next few years. Reusing materials from used LIBs can reduce possible material shortages.

However, despite significant progress in LIBs recycling, the use of graphite from used batteries lags behind the recycling and use of cathode materials [12]. The economic feasibility of processing a graphite anode is also confirmed by the fact that various contaminants present in natural grades of graphite prevent its direct use as a LIB anode. As a rule, the production of battery graphite includes several stages, including mining, beneficiation, purification and processing [13]. All these stages lead to significant environmental pollution and pose a risk to human health. A significant, albeit less well-known, aspect is that 1 kg of graphite is needed to produce 1 kWh of commercial LIB capacity [14]. Given that the graphite content in LIB ranges from 12 to 21 percent by weight (depending on the type of battery), graphite production from spent LIB can be considered as an alternative method for obtaining graphite for LIBs [12,15].

In this study, we present a way to recycle graphite anode, together with some physicochemical and electrochemical parameters of the reduced graphite obtained during the processing of a lithium iron phosphate battery.

Experimental

The source of spent graphite in our studies was the anode of lithium iron phosphate battery HWE200A, LF54174200 3.2 V 200 Ah (China) [16]. The reasons for the failure of this battery were an internal short circuit due to thermal runaway, as evidenced by the lack of voltage between the battery terminals, and partially fused and burned electrodes.

According to *Zhang et al.* [17], spent graphite containing various impurities has a lower initial discharge capacity of 298.7 mA·h/g compared to the capacity of 354.2 mA·h/g for the original battery graphite. Note that the theoretical capacity of high-purity graphite (99.99 %) is 372 mA·h/g.

To restore the original properties of spent graphite, it is very important to remove residual impurities from it. For this purpose, we used diluted solutions of nitrate acid. As shown by Barsukov *et al.* [18], the treatment of natural flake graphite in nitric acid solutions makes it possible to remove almost all metal impurities with the exception of silicon and aluminum compounds. The latter are extracted either by sintering with alkali [18] or HF [19] or by high-temperature treatment at 3000 °C. The advantage of spent graphite material is that silicon and aluminum compounds have already been extracted earlier, at the stage of purification of natural graphite to the level of 99.95 % C. Therefore, the treatment of spent graphite in nitric acid may be quite sufficient to remove any metal impurities.

The battery was mechanically disassembled to separate the cathode, anode, and separator. The anode, a graphite-based electrode mass deposited on both sides of copper foil, was cut into small pieces and placed in a 20 % nitric acid solution. The ratio of the solid to liquid phase was 1:12. After the copper was completely dissolved, the solution turned blue, indicating the formation of copper (II) nitrate. The treatment of the graphite anode in nitric acid made it possible not only to separate the carbon material of the anode from the copper foil but also to get rid of the solid electrolyte film (SEI) on its surface. A mixture of graphite, acetylene soot and polymer binder glue remained as an insoluble precipitate. In order to grind and more completely extract the impurities present in the graphite anode, the resulting suspension was subjected to ultrasonic treatment on the disperser XM-650DT (China) for 20 minutes. After separating the sediment, the latter was repeatedly washed with distilled water to a pH 7. In order to remove the polymer binder and amorphous carbon impurities from the graphite anode, the resulting sample was annealed for 2 h at 700 °C. The heating and cooling rate of the furnace was 5° min^{-1}. After cooling, the resulting material was crushed and sifted through a sieve with a mesh size of 40 μm.

The method for determining the ash content of graphite was based on the process of calcination of certain quantities of graphite and weight analysis of the ash residue. To do this, 2 grams of

graphite were placed in a crucible and heat treated in a muffle furnace for eight hours at 1050 °C. After calcination, the crucibles were removed from the muffle, cooled for 10 minutes on a metal plate, and then placed in a desiccator without a desiccant for further cooling. At the final stage, the ash residue was weighed on analytical balances. According to the analysis of a series of three crucibles, the ash content of regenerated graphite from LIB did not exceed 0.02 %.

It should be noted that in addition to copper nitrate, the solution contains a certain amount of lithium nitrate, which was formed as a result of the dissolution of the solid-electrolyte film from the surface of the graphite anode. The results of atomic emission flame spectrometry of the solution (Shimadzu AA-6300, Japan) for the residual lithium content show a value of 430 ± 5 mg/l. To do this, an excessive amount of sodium hydroxide is added to the solution in order to obtain an insoluble precipitate of copper (II) hydroxide. After separating the latter, sodium carbonate was added to the resulting solution and evaporated. Due to the weak solubility of lithium carbonate in water, it precipitates during evaporation. This method is the main method for obtaining lithium carbonate in the processing of cathode materials [20].

The scheme of graphite anode processing is shown in Figure 2.

Figure 2. *The scheme of graphite anode processing*

The phase composition, morphology, and particle size of reduced graphite were analyzed by X-ray diffraction (Dron-4-07, LOMO, Russia, Co-K_α radiation) and scanning electron microscopy (JSM-6700f, JEOL, Japan) methods.

Electrochemical tests were done using a half-cell with a working graphite electrode and lithium as the reference and counter electrodes. Working electrodes consist of 94 wt.% of the graphite, 1 wt.% of the conductive additive (soot) and 5 wt.% of the water-soluble binder (NV-1T, “Casnovo” corporation, China).

The suspension of the composite electrode was prepared by mixing the starting materials on an IKA RW 20 mixer for 50 minutes. The resulting suspension was applied to copper foil by a doctor blade method with the 80 µm thickness. The porosity of the electrode was determined by the ratio of the crystallographic density of graphite (~2.16 g/cm^3) to the measured density of the electrode material.

The parameters of the obtained electrodes, after drying and pressing, are shown in Table 1.

Table 1. *Parameters of graphite electrodes*

Sample	Electrode mass, g	Mass of graphite, g	Electrode thickness, µm	Porosity, %
1	0.006	0.0048	30±5	54
2	0.007	0.0063	40±5	56

CR2032-type coin cells were assembled using the dried anode and Celgard 2500 as a separator in a glove box. The electrolyte used in this study was 1M $LiPF_6$ in a mixture of ethylene carbonate and dimethyl carbonate, both at a volume ratio of 1:1. A lithium disk of 16 mm in diameter served as both the reference and counter electrode in the cell assembly. Galvanostatic studies of these cells were conducted using the Neware BTS 4000 battery analyzer (China). Additionally, electrochemical impedance spectroscopy (EIS) was performed with an Autolab PGSTAT 302 (Switzerland). The impedance spectra obtained were subsequently analyzed using Nova 2.1 software. EIS measurement were taken between 1 MHz to 0.01 Hz with a voltage amplitude of 5 mV after full lithiation of the graphite electrode (0.01 V *vs.* Li/Li^+ electrode).

Results and discussion

As known, graphite has a layered, planar structure. In each layer, the carbon atoms are arranged in a honeycomb lattice with a bond length of 0.142 nm, and the distance between planes is 0.335 nm [21].

Figure 3 shows the X-ray diffraction pattern of purified graphite prepared according to the scheme proposed above, which has well structural and phase purity. The XRD of graphite possesses three signature peaks at 26.3° (002), 44.2° (100) and 54.5° (004). The peak at 2θ = 26.3° indicates well-organized structure of graphite with an interlayer spacing of 0.338 nm. This layer spacing is in agreement with the spacing in graphite. The broad peak at 2θ = 44.2° is attributed to the presence of some defects [22].

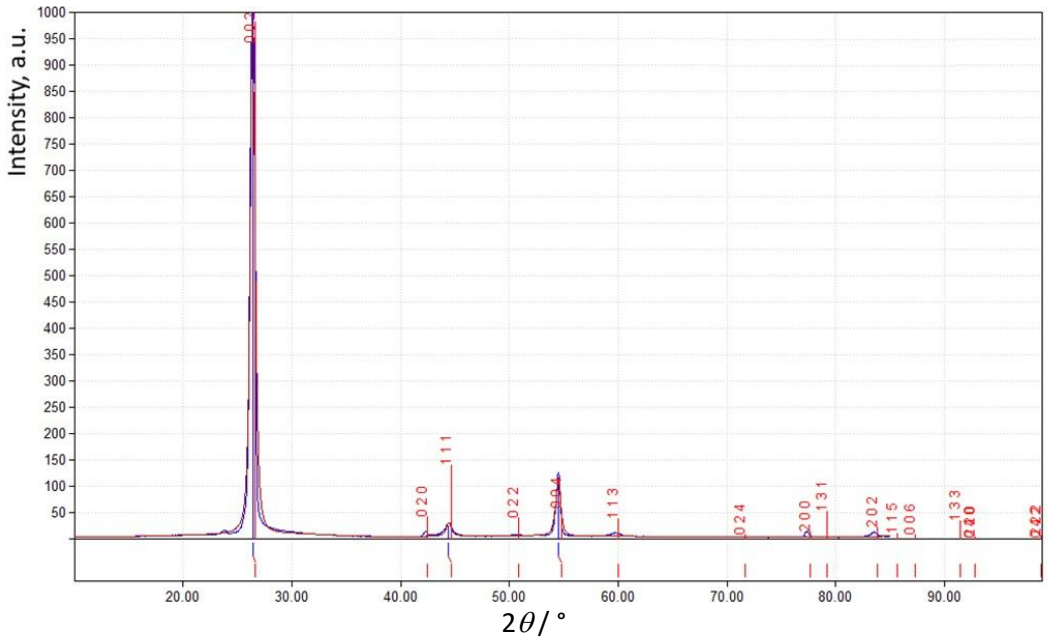

Figure 3. *XRD pattern of purified graphite*

Figure 4 represents the SEM image of purified graphite. As can be observed, well-defined sheets of graphite 1-3 μm in diameter are presented.

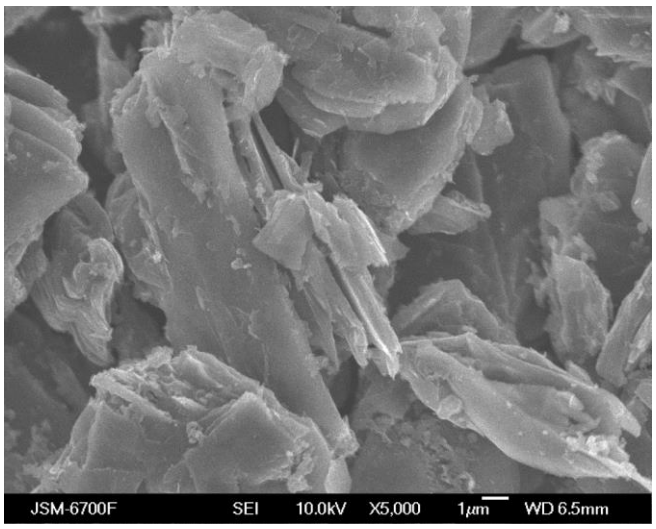

Figure 4. *SEM image of purified graphite*

On the galvanostatic curve of the 1st charge/discharge cycle of a graphite electrode (Figure 5), it can be noted that there is an irreversible capacity of about 40 mA·h/g, which can be attributed to the formation of SEI on its surface. In addition, there are three small plateaus at potentials below 0.2 V relative to Li^+/Li during the cathode sweep. These plateaus are caused by the insertion of lithium ions into the layered graphite structure and transformations between different stages of intercalation compounds from the LiC_{36} stage to the LiC_6 stage, respectively [23,24].

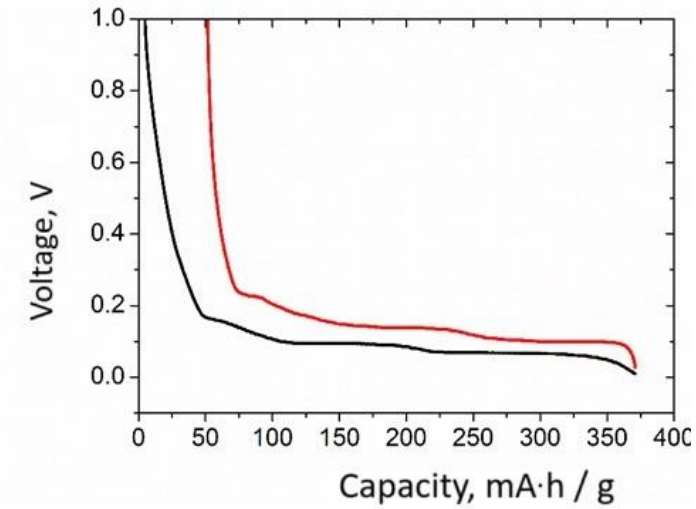

Figure 5. *Changing the profile of the charge/discharge curve of the 1st cycle of the graphite electrode (sample 1): black – charge, red – discharge. Current rate is 0.05C (I = 0.089 mA)*

During the anodic sweep, three plateaus are also observed, which relate to the deintercalation of lithium ions from the graphite electrode. An increase in the intercalation/deintercalation current rate of lithium ions leads to a slight decrease in the specific capacitance of the electrode (Figure 6) at current values not exceeding 0.2 C (1-3 cycle - current rate was 0.05C; 4-9 cycles - 0.1C; 10-19 cycles - 0.2C) and increase coulombic efficiency during cycling. A further increase in the discharge current rate to values of 0.5C leads to a more significant decrease in the specific capacity of the graphite electrode. This can be observed in Figure 6 (cycles: 20-29) due to limitations in the intercalation of lithium ions between the graphite layers. Thus, when using the constant current-constant voltage (CCCV) mode or reducing the intercalation current of lithium ions to 0.1 C, higher currents can be realized during subsequent de-insertion (Figure 7).

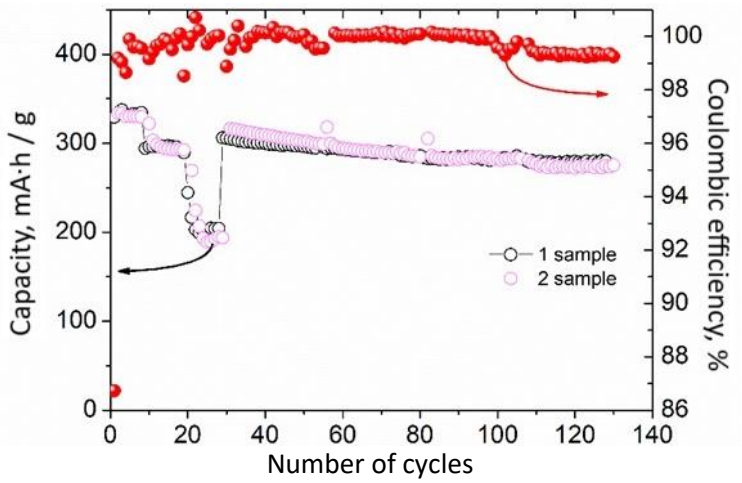

Figure 6. *Change in specific capacity and Coulomb efficiency of the graphite electrode during cycling. Current rate:* I *= 0.05 C (cycles 1-3);* I *= 0.1 C (cycles 4-9);* I *= 0.2 C (cycles 10-19);* I *= 0.5 C (cycles 20-29);* I *= 0.2 C (cycles 30-130)*

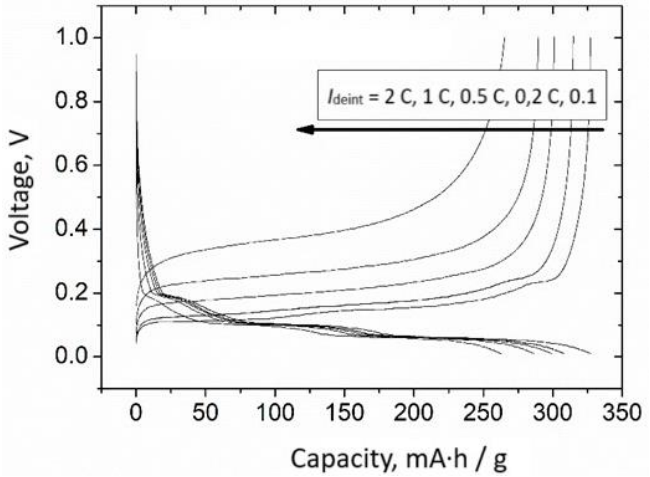

Figure 7. *Galvanostatic cycling curves of the graphite electrode depending on the current rate in the range:* $I_{int.}$ *= 0.1 C (const.);* $I_{deint.}$ *= 0.1 – 2.0 C*

Upon cycling of the graphite anode, an increase in coulombic efficiency is observed during the initial 20 cycles, after which it stabilizes, reaching approximately 99.2±0.2 %. This effect can be attributed to the reduced contribution of irreversible capacitance, which is associated with the formation and compaction of the solid electrolyte interface (SEI) on the surfaces of both the working and counter electrodes. However, increasing the current rate to 0.5 C during cycles 20 to 30 results in a marked decrease in specific capacitance, dropping to about 200 mA·h/g. Subsequently, lowering the intercalation/deintercalation current rate to 0.2C helps to restore the capacity values to around 300 mA·h/g. Despite this recovery, a slight decline in capacity is observed with further cycling, extending from cycles 30 to 130. The gradual decrease in the capacity of the graphite electrode over these cycles is illustrated in Figure 8.

Here, it is worth noting that in the process of cycling, there is a decrease in the average voltage at the insertion of lithium ions into graphite on each of the "shelves" at cathodic polarization and an increase in the average voltage at de-insertion of lithium ions – at anodic polarization, which indicates an increase in the internal resistance of the cell. First of all, the increase in internal resistance should be attributed to the formation of a dense SEI on the lithium electrode. This assumption is also evidenced by impedance hodographs (Figure 9) obtained on the 30th and 130th cycles at the potential of 0.01 V.

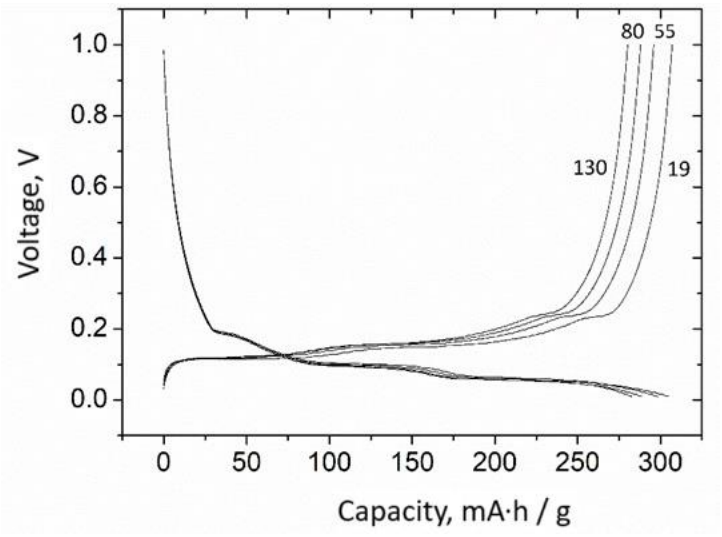

Figure 8. *Changing the profile of the charge/discharge curves during the cycling of the graphite electrode. Current rate is 0.2 C. Numbers indicate cycle numbers*

To describe the processes occurring during the silencing of the electrode, several equivalent circuits have been proposed. For instance, *Wang et al.*[25] interpret changes in the appearance of impedance hodographs in terms of five possible processes. In another study [26], simpler schemes are proposed to describe the resistance of the electrochemical system to the alternating current flowing through it.

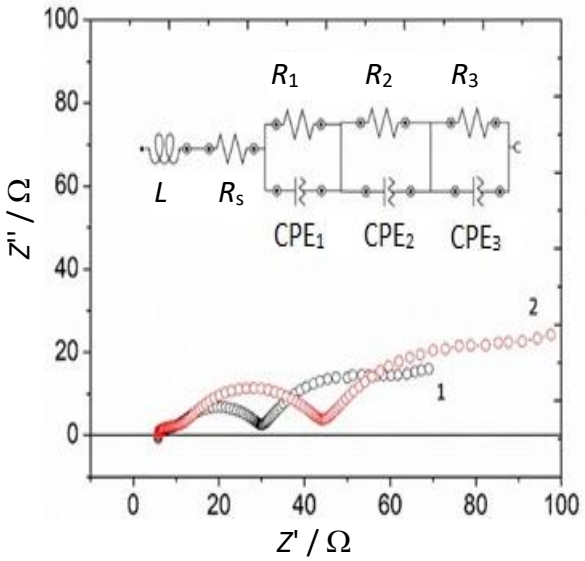

Figure 9. *Nyquist diagram and equivalent electrical circuit of a graphite electrode (sample 1) 1 - 30th cycle; 2 - 130th cycle*

The equivalent electrical circuit from Figure 9 describes the processes in Table 2.

Table 2. *The process explains the equivalent electrical circuit*

No	Process	Frequency area
1	Inductive wiring of metal contacts (L_0)	High (10 to 0.1 MHz)
2	Resistance of electrolytes in the pores of the separator (Celgard 2500) (R_S)	
3	Charge transfer through the SEI on a graphite electrode	Middle (100 to 0.01 kHz)
4	Charge transfer through the SEI/metallic lithium	Low (1.00 to 0.01 Hz)
5	Diffusion of lithium ions compatible with adsorption into the structure of the material	

However, it is important to note that since the impedance hodographs of the elements are obtained after full lithiation of the graphite electrode, the classical Warburg impedance, typically represented as an inclined line at a 45° angle, transforms into a semicircle. This semicircular shape is characteristic of porous and rough surfaces. Consequently, to accurately describe the equivalent circuit in this scenario, a parallel connection composed of a resistance (R_3) and a distributed capacitance (CPE_3) was utilized in place of the Warburg diffusion impedance. The values for the elements obtained using this revised equivalent circuit model are presented in Table 3.

Table 3. *Values of some electrical equivalent circuit parameters*

Sample	Number of cycles	L_0 / H	R_S / Ω	R_1 / Ω	R_2 / Ω	R_3 / Ω
1	30	$270 \cdot 10^{-9}$	5.85	6.06	20.6	45.6
2	130			9.24	33.9	75.4

The values of inductance (L_0) and electrolyte resistance in the separator pores (R_S) practically do not change during cycling. The resistance to charge transfer through SEI on the graphite electrode (R_1) increases by ~30 % over 95 cycles from 6.06 to 9.24 Ω. However, the greatest contribution to the increase in charge transfer resistance through SEI falls on the lithium counter electrode (R_2), which increases by 13 Ω.

Conclusions

In conclusion, the anode material retrieved from a malfunctioning lithium iron phosphate battery, primarily composed of graphite, acetylene black, and a polymer-based adhesive, presents a significant recycling potential. The direct reutilization of this material in lithium-ion batteries without prior purification is not feasible due to its diminished electrochemical properties, largely attributable to the presence of impurities. To address this, a two-stage regeneration process is employed. Initially, the anode material undergoes treatment in a nitric acid solution, effectively removing the copper foil and extracting lithium ions, as well as other electrolyte interaction byproducts accumulated during the battery's operational life. This is followed by a thermal treatment, which is essential for eliminating the acetylene soot and decomposing the polymer binder. The efficacy of this regeneration process is underscored by the experimental results, wherein the specific capacity of the recycled graphite is recorded at approximately 330 mA·h/g at 0.1 C discharge rate. These values are not only on par with commercially available graphite but also meet the requisite standards for reuse in LIBs, thereby underscoring the viability of this recycling approach.

Acknowledgements*: The work was carried out with the support of the National Research Foundation of Ukraine within the framework of the project "Development of new types of high-capacity solid-state lithium batteries to ensure the energy security of Ukraine" (ID 2022.01/0154).*

Conflict of interest*: The authors declare no conflict of interest.*

References

[1] M. Li, M. Li, J. Lu, Z. Chen, K. Amine, 30 Years of lithium-ion batteries, *Advanced Materials* **30** (2018) 1800561. https://doi.org/10.1002/adma.201800561

[2] J. Xie, Y. Lu, A retrospective on lithium-ion batteries, *Natural Communication* **11** (2020) 2499. https://doi.org/10.1038/s41467-020-16259-9

[3] X. Feng, R. Dong, T. Wang, Q. Zhang, Ab-initio simulations accelerate the development of high-performance lithium sulfur batteries, *Material Lab,* **1** (2022) 220031. https://doi.org/10.54227/mlab.20220031
[4] Y. Qiao, H. Zhao, Y. Shen, L. Li, Z. Rao, G. Shao, Y. Lei, Recycling of graphite anode from spent lithium-ion batteries: Advances and perspectives, *EcoMat* **5** (2023) e12321. https://doi.org/10.1002/eom2.12321
[5] T. Hettesheimer, C. Neef, S. Link, T. Schmaltz, F. Schuckert, A. Stephan, M. Stephan, T. Wicke, *Lithium-Ion Battery Roadmap – Industrialization Perspectives Toward 2030,* Fraunhofer Institute for Systems and Innovation Research ISI, Karlsruhe, Germany, 2023. https://doi.org/10.24406/publica-2153
[6] Fraunhofer ISI Meta-Market-Monitoring, https://metamarketmonitoring.de/ (Accessed on December 25, 2023).
[7] Battery Materials Review the 2024. Yearbook the state of play in battery materials, https://www.batterymaterialsreview.com/ (Accessed on December 25, 2023)
[8] X. T. Wang, Z. Y. Gu, E. H. Ang, X. X. Zhao, X. L. Wu, Y. Liu, Prospects for managing end-of-life lithium-ion batteries: present and future, *Interdisciplinary Materials* **1** (2022) 417-433. https://doi.org/10.1002/idm2.12041
[9] S. Natarajan, M. L. Divya, V. Aravindan, Should we recycle the graphite from spent lithium-ion batteries? The untold story of graphite with the importance of recycling, *Journal of Energy Chemistry* **71** (2022) 351-369. https://doi.org/10.1016/j.jechem.2022.04.012
[10] X. Zeng, M. Li, D. A. El Hady, W. Alshitari, A. S. Al-Bogami, J. Lu, K. Amine, Commercialization of lithium battery technologies for electric vehicles, *Advanced Energy Materials* **9** (2019) 1900161. https://doi.org/10.1002/aenm.201900161
[11] B. Scrosati, J. Garche, Lithium batteries: status, prospects and future, *Journal of Power Sources* **195** (2010) 2419-2430. https://doi.org/10.1016/j.jpowsour.2009.11.048
[12] B. Moradi, G. G. Botte, Recycling of graphite anodes for the next generation of lithium ion batteries, *Journal of Applied Electrochemistry* **46** (2016) 123-148. https://doi.org/10.1007/s10800-015-0914-0
[13] T. C. Wanger, The lithium future-resources, recycling, and the environment, *Conservation Letters* **4** (2011) 202-206. https://doi.org/10.1111/j.1755-263X.2011.00166.x
[14] S. Natarajan, V. Aravindan, An urgent call to spent LIB recycling: whys and wherefores for graphite recovery, *Advanced Energy Materials* **10** (2020) 2002238. https://doi.org/10.1002/aenm.202002238
[15] P. Perumal, B. Raj, M. Mohapatra, S. Basu, Sustainable approach for reclamation of graphite from spent lithium-ion batteries, *Journal of Physics: Energy* **4** (2022) 045003. https://doi.org/10.1088/2515-7655/ac8a17
[16] 3.2 V 200 A·h Prismatic Deep Cycle $LiFePO_4$ Rechargeable Solar Batteries, https://howellenergy.en.made-in-china.com/product/vOjnfzCVlDkq/China-3-2V-200ah-Prismatic-Deep-Cycle-LiFePO4-Rechargeable-Solar-Batteries.html (Accessed on December 15, 2023)
[17] J. Zhang, X. Li, D. Song, Y. Miao, J. Song, L. Zhang, Effective regeneration of anode material recycled from scrapped Li-ion batteries, *Journal of Power Sources* **390** (2018) 38-44. https://doi.org/10.1016/j.jpowsour.2018.04.039
[18] V. Barsukov, V. Lysin, V. Khomenko, K. Lykhnitskii, Yu. Skrypnyk, *Method for chemical purification of graphite,* Ukrainian patent for a utility model No. 56888. Jan. 25 (2011)
[19] V. Barsukov, V. Lysin, V. Khomenko, K. Lykhnitskii, Yu. Skrypnyk, *Method for chemical purification of graphite,* Ukrainian patent for a utility model No. 98691. June 11 (2012)

[20] N. Fatima, N. Solangi, F. Safdar, J. Kumar, A short overview of recycling and treatment of spent $LiFePO_4$ battery, *North American Academic Research* **5** (2022) 76-87. https://doi.org/10.5281/zenodo.6970023
[21] Y. Sheng, X. Tang, E. Peng, J. Xue, Graphene Oxide Based Fluorescent Nanocomposites for Cellular Imaging, *Journal of Material Chemistry B* **1** (2013) 512-521. https://doi.org/10.1039/c2tb00123c
[22] Y. Wu, B. Wang, Y. Ma, Y. Huang, N. Li, F. Zhang, Y. Chen, Efficient and Large-Scale Synthesis of Few-Layered Graphene Using an Arc-Discharge Method and Conductivity Studies of the Resulting Films, *Nano Research* **3** (2010) 661-669. https://doi.org/10.1007/s12274-010-0027-3
[23] Z. X. Shu, R. S. McMillan, J. J. Murray, Electrochemical Intercalation of Lithium into Graphite, *Journal of The Electrochemical Society* **140** (1993) 922-927. https://doi.org/10.1149/1.2056228
[24] V. A. Sethuraman, L. J. Hardwick, V. Srinivasan R. Kostecki, Surface Structural Disordering in Graphite upon Lithium Intercalation/Deintercalation, *Journal of Power Sources* **195** (2010) 3655-3660. https://doi.org/10.1016/j.jpowsour.2009.12.034
[25] C. Wang, A. J. Appleby, F. E. Little, Electrochemical impedance study of initial lithium ion intercalation into graphite powders, *Electrochimica Acta* **46** (2001) 1793-1813. https://doi.org/10.1016/S0013-4686(00)00782-9
[26] R. Yazami, Y. F. Reynier, Mechanism of self-discharge in graphite–lithium anode, *Electrochimica Acta* **47** (2002) 1217-1223. https://doi.org/10.1016/S0013-4686(01)00827-1

1 *J. Electrochem. Sci. Eng.* **00(0)** (2023) S00-S00

2
3 Open Access : : ISSN 1847-9286
4 www.jESE-online.org

5 **Supplementary material to**

6